# IMU-based sensor-to-segment multiple calibration for upper limb joint angle measurement? a proof of concept

Mahdi Zabat, Amina Ababou, Noureddine Ababou, Raphaël Dumas

post-print : ZABAT, Mahdi, ABABOU, Amina, Ababou, Noureddine, DUMAS, Raphaël, 2019, IMU-based sensor-to-segment multiple calibration for upper limb joint angle measurement? a proof of concept, Medical & Biological Engineering & Computing, 57, 11, Springer Verlag, pp. 2449-2460, DOI: 10.1007/s11517-019-02033-7

# IMU-based Sensor-to-Segment Multiple Calibration for Upper Limb Joint Angle Measurement - A proof of concept

M. Zabat[a], A. Ababou[a], N. Ababou[a], R. Dumas[b]

[(a)]Laboratory of Instrumentation, University of Science and Technology Houari Boumediene, Algiers, Algeria

[(b)] Univ Lyon, Université Claude Bernard Lyon 1, IFSTTAR, LBMC UMR_T9406, F69622, Lyon, France.

Revised manuscript (16/06/2019)

## Abstract

A lot of attention has been paid to wearable inertial sensors regarded as an alternative solution for outdoor human motion tracking. Relevant joint angles can only be calculated from anatomical orientations, but they are negatively impacted by soft tissue artifact (STA) defined as skin motion with respect to the underlying bone; the accuracy of measured joint angle during movement, is affected by the ongoing misalignment of the sensor. In this work, a new sensor-to-segment calibration using IMUs is proposed. Inspired by the multiple calibration for a cluster of skin markers, it consists in performing first multiple static postures of the upper limb in all anatomical planes. The movements that affect sensors alignment are identified then alignment differences between sensors and segment frames are calculated for each posture and linearly interpoled. Experimental measurements were carried out on a mechanical model and on a subject who performed different movements of right elbow and shoulder. Multiple calibration showed significant improvement in joint angle measurement on the mechanical model as well as on human joint angle comparing to those obtained from attached sensors after technical calibration. During shoulder internal-external rotation, the maximal error value decreased more than 50% after correction.

Keywords — Joint angle; IMU measurement; Posture; Calibration; Soft-tissue artifact

## Nomenclature

$p_i^0$: Segment i orientation at neutral posture 0

$q_i^0$: Sensor i frame orientation at neutral posture 0

$\tilde{q}_1^0$: Rotation of IMU1 at posture 0 to align with gravity

$p_i^j$: Segment i orientation at posture j

$q_i^j$: Sensor i orientation at Posture j

$\tilde{p}_i^j$: 90°-rotation about a given axis of the segment i at posture j

$\tilde{q}_i^j$: Alignment difference between $q_i^j$ and $p_i^j$

$\bar{\tilde{q}}_i^{\mathbf{u},\alpha}$: Mean value of all alignment differences $\tilde{q}_i^j$ calculated for each segment i at all postures j resulting either from the rotation of the joint angle α=0° or 90° about the axis **u** and presenting the same segment frame orientation.

$\bar{\tilde{q}}_i^{\mathbf{u}}(\theta)$: Alignment correction during movement and obtained by linear interpolation

$\bar{\tilde{q}}_i^{\mathbf{u},\mathbf{v}}(\theta_1, \theta_2)$: Alignment correction during movement and obtained by bilinear interpolation

$p_i$: corrected segment frame orientation

## 1. Introduction

Several non-invasive technologies can be used to assess human joint angles such as electrogoniometers [1], inertial measurement units IMUs [2-5] and optical motion capture system (OMCS) system [6, 7] considered as gold-standard. From a practical point of view, OMCS system cannot be easily used for daily rehabilitation activities because of the cumbersome protocol and calibration procedure, limited working space, and so on. OMCS system is typically used in the laboratory to evaluate the accuracy of other (ambulatory) measurement systems [3, 5].

Significant attention has been paid to IMUs regarded as alternative tools for human motion tracking which can provide low-cost ambulatory measurements and easy set up compared to OMCS. When using these motion tracking technologies to estimate human joint angles, two sources of errors can appear and affect measurement correctness. The first one is related to the measurement system itself [8, 9] while

the other results from the sensors misalignment with respect to human segments [4, 10-14]. What is more, the sensor misalignment is changing during the movement due to soft tissue artifact (STA) [7, 15-19]. STA is defined in the literature as the skin motion relative to the underlying bone [7, 20] and is regarded as a major source of error that disrupts the estimation of joint angles when non-invasive measurement systems are used [21]. In OMCS measurements, STA results in markers cluster shape deformation as well as, predominantly, maker-cluster rotation and translation with respect to the underlying bone. Several papers have been reported in the literature on how to compensate STA effects to improve the accuracy of joint angles measurements. A multiple calibration procedure was proposed to model OMCS marker-cluster deformation between a set of calibration postures in knee flexion/extension [7, 19] or scapular movement [22]. Typically, in double calibration, the alignment difference is assessed for two calibration postures. A linear interpolation in time is implemented on the position of anatomical landmarks in the technical frame [7, 22]. STA was defined in [15] as a series of rigid geometrical transformations and a dynamic calibration based on an ad hoc model was applied. The compensation of STA effects related to skin-mounted markers placed on upper or lower limb has been extensively studied in the literature, and some efficiency has been proved when using multiple calibration of the clusters of markers [7, 17, 19, 22]. As for OMCS, IMU calibration procedure consists in establishing a relation between the sensor frame and the segment frame related to the underlying bone [2-4, 20, 23-30]. This procedure named “sensor-to-segment calibration” can either be one-axis [30] or three-axis calibration [2-4, 10]. Generally, static calibration is performed by asking the subject to maintain postures in order to establish the relation between the sensor and the segment frames. In the case of IMU-calibration, the alignment difference between the sensor frame and the segment frame was supposed constant in time. This is a classical assumption made in most studies on sensor-to-segment calibration. In the case of joint angle measurement by IMUs, two adjustments based on the mean misalignment were proposed by Meng et al. [20] with multiple static postures related to five active movements such that only one angle was varied per movement. It is important to keep in mind that they combined both IMU and OMCS to get a statistics of the alignment difference. The latter was not modeled individually but in average using a linear regression of data collected from fifteen participants

including the body fat percentage. They obtained values less than 1° for mean error, RMSE and SD after adjustments. A multiple calibration method that do not refer to OMCS is yet to be developed for IMUs.

In this paper, an IMU-based sensor-to-segment calibration referred to as multiple calibration for upper limb joint angle measurement is proposed to take into account the variation of the misalignment between sensor and segment. It consists in performing multiple static postures during the calibration session. The movements that affect IMUs alignment (i.e. sensor frame orientation vs. segment frame orientation) are identified by calculating the alignment differences at the two joint angles (0° and 90°) for each joint axis of movement. Then, linear or bilinear interpolation is applied between this two alignment differences to assess this difference during the movement. To the author's knowledge, such a method of misalignment compensation has not been reported in the literature. In the following, Section 2 introduces first the calibration postures and the method of calculation and correction of the misalignment between segment and IMU orientations. Section 3 presents the results of the tests performed on mechanical model and on human right upper limb. A discussion of the achieved results is provided in Section 4. Finally, Section 5 draws conclusions.

## 2. Materials and Methods

Four IMUs are placed on the right upper limb and the thorax as shown in Fig.1. A so-called technical calibration [4] is first performed by adjusting manually IMUs positions in order to visually align their local frames with the associated segment anatomical frames. Then, static calibration is achieved at several predefined static postures.

### 2.1. Calibration postures

Twenty-one static predefined postures were selected in the proposed multiple calibration procedure. Starting from the anatomical posture presented in Fig. 1, the subject has to perform the other twenty static postures illustrated in Fig. 2. These postures were selected in order to cover simple anatomical upper limb joints movements such as flexion/extension (FE), adduction/abduction (AA), and internal/external rotation (IER) in the three anatomical planes or any combination of them.

FIGURE 1 HERE

FIGURE 2 HERE

The calibration postures illustrated in Fig. 2 are the results of either 0°-rotation or 90°-rotation of distal segment with respect to a proximal segment of the right upper limb. It is much easier for a subject to perform rotations of 0 or 90 degrees than any other prescribed joint angles values. In this work, the joint angles are supposed to remain 0° or vary by 90°, and the calibration postures are only be considered at these two rotation angle values during the calibration session.

## 2.2. Initial alignment and Alignment differences

Both segment and IMUs frame orientations must be defined at each one of the proposed calibration postures of Fig. 2. In this paper, quaternion representation was used to describe the orientations.

The IMUs frames as well as segment frames of the upper limb and the thorax in neutral posture are shown in Fig. *3a and b*. In this work, the quaternions q and p are related to the IMUs frames orientations and segment frames orientations, respectively. In a first stage, considering the technical calibration [4] established during the neutral posture 0, the orientations of both sensors and segments frames are assumed to be aligned, except for the thorax. For this segment, the gravity axis is used to re-aligne the vertical axis of the sensor:

$$p_i^0 = q_i^0 \quad \text{for } i=2,3,4 \quad \text{and} \quad p_1^0 = \tilde{q}_1^0 \, q_1^0 \quad \text{for } i = 1 \tag{1}$$

with $p_i^0$ ($i$ from 1 to 4 for thorax to hand) the segment frame orientation and $q_1^0$ the sensor frame orientation in posture 0. The quaternion $\tilde{q}_1^0$ represents rotation of IMU1 at posture 0 illustrated in Fig. 3a that transforms the IMU1 frame orientation so that it coincides with the thorax frame in Fig.3b.

In the posture 0, after this calibration, all the segment definitions are expected to follow, at best, ISB recommendations [31]. The right-arm and thorax segment frames have their X, Y and Z axes pointing forward, upward and to the right, respectively.

FIGURE 3 HERE

During all the calibration session, the thorax remains static and all upper limb movements are performed with respect to the thorax segment frame considered as a reference. The movements from the neutral posture (posture 0) to the postures adopted for the calibration are then interpreted as known rotation noted $\widetilde{p}_i^j$ (90° about a given axis) of the segment frames with respect to the thorax. For instance, the right upper limb segment frames' orientations shown in Fig. 3 are related with two calibration postures. Posture 3 segment orientations illustrated in Fig. 3c are deduced from 90° clockwise rotations about the X-axis of the thorax segment frame. The segment frame orientations of the upper arm, forearm, and hand represented by the quaternion $p_i^j$ are therefore calculated using the relation (2).

$$p_i^j = \widetilde{p}_i^j \; p_I^0 \tag{2}$$

The subscript *i* (from 2 to 4) corresponds to upper limb segments while the superscript *j* represents the different calibration postures (from 1 to 21).The segment orientations corresponding to all the calibration postures are obtained using a similar procedure. At the end of the calibration session, two kinds of upper limb segment frame orientations are gotten, i.e., the calibrated orientations $p_i^j$ deduced from thorax frame orientation and the directly measured orientations $q_i^j$ estimated from the IMUs. Due to STA, the calibrated and directly measured orientation are not identical, so the alignment difference $\widetilde{q}_i^j$ between $q_i^j$ and $p_i^j$ can be calculated for each segment involved in a calibration posture. The alignment difference $\widetilde{q}_i^j$ related to a given calibration posture *j* is defined by

$$\widetilde{q}_i^j = p_i^j \; q^{*}{}_i^j \tag{3}$$

with $q^{*}{}_i^j$ is the quaternion conjugate of the quaternion $q_i^j$.

## 2.3. Correction of IMU frame orientation

For a given segment *i*, the same segment frame orientation $p_i^j$ may be present in more than one posture *j*, so the alignment difference related to that specific segment will be the mean value of all alignment differences $\tilde{q}_i^j$ calculated at all postures presenting the same segment frame orientation.

$$\bar{\tilde{q}}_i^{\mathbf{u},\alpha} = \frac{\sum_{j=1}^{n} \tilde{q}_i^j}{n} \tag{4}$$

with *n* the number of postures presenting the same segment frame orientation. These postures result from either $\alpha = 0°$ or $\alpha = 90°$ rotation about one axis of the thorax frame. Thus, for each joint rotation axis **u**, and each of these rotations, a mean alignment difference is computed. Moreover, for each movement about a joint axis **u**, $\bar{\tilde{q}}_i^{\mathbf{u},0}$ and $\bar{\tilde{q}}_i^{\mathbf{u},90}$ correspond to the average alignment difference values calculated when joint angle $\theta$ is equal to 0° and 90°, respectively. For example, in elbow FE movement about the axis $\mathbf{u} = \mathbf{Z}_{aU}$, the alignment difference value $\bar{\tilde{q}}_i^{\mathbf{u},0}$ for the elbow fully extended ($\theta = 0°$) is taken as the mean value of the alignment difference values related to the five postures 1, 2, 3, 20 and 21 shown in Fig. 2 and obtained using Eq. (4). In the same way, the alignment difference value $\bar{\tilde{q}}_i^{\mathbf{u},90}$ related to 90° elbow flexed is obtained from the mean value of the alignment difference values associated with postures 4 to 19 of the same figure.

Linear interpolation is applied between $\bar{\tilde{q}}_i^{\mathbf{u},0}$ and $\bar{\tilde{q}}_i^{\mathbf{u},90}$ and the alignment difference value $\bar{\tilde{q}}_i^{\mathbf{u}}(\theta)$ during the movement is given by

$$\bar{\tilde{q}}_i^{\mathbf{u}}(\theta) = \bar{\tilde{q}}_i^{\mathbf{u},0} + \frac{\bar{\tilde{q}}_i^{\mathbf{u},90} - \bar{\tilde{q}}_i^{\mathbf{u},0}}{90} \cdot \theta \tag{5}$$

Therefore, the segment frame orientation $p_i$ of the segment i is computed from the IMU frame orientation $q_i$ corrected by the alignment difference $\bar{\tilde{q}}_i^{\mathbf{u}}(\theta)$ obtained from the proposed multiple calibration. The corrected segment frame orientation $p_i$ is related to $q_i$ according to the Eq. (6).

$$p_i = \bar{\tilde{q}}_i^{\mathbf{u}}(\theta)\, q_i \tag{6}$$

with $\theta$ the joint angle obtained about axis **u** after technical calibration (i.e., computed from $q_i$ ).

The joint angles were finally computed following the ISB convention [31] considering the relative movement of the distal segment with respect to the proximal segment. The YZY sequence is used to estimate shoulder joint angles while the ZXY sequence is used for elbow. In other words, shoulder IER corresponds to $\mathbf{u} = \mathbf{Y}_{aU}$ and elbow FE and PS correspond to $\mathbf{u} = \mathbf{Z}_{aU}$ and $\mathbf{u} = \mathbf{Y}_{aF}$, respectively.

In case the alignment difference $\widetilde{\bar{q}}_i^{\mathbf{u}}$ depends on the variation of both two joint angles $\theta_1$ and $\theta_2$, bilinear instead of linear interpolation is applied; the related alignment difference is expressed by:

$$\bar{\tilde{q}}_i^{\mathbf{u},\mathbf{v}}(\theta_1,\theta_2) = \frac{(\bar{\tilde{q}}_i^{\mathbf{u},90,\mathbf{v},0} - \bar{\tilde{q}}_i^{\mathbf{u},0,\mathbf{v},0})}{90}.\theta_1 + \frac{(\bar{\tilde{q}}_i^{\mathbf{u},0,\mathbf{v},90} - \bar{\tilde{q}}_i^{\mathbf{u},0,\mathbf{v},0})}{90}.\theta_2 + \frac{(\bar{\tilde{q}}_i^{\mathbf{u},0,\mathbf{v},0} - \bar{\tilde{q}}_i^{\mathbf{u},0,\mathbf{v},90} + \bar{\tilde{q}}_i^{\mathbf{u},90,\mathbf{v},90} - \bar{\tilde{q}}_i^{\mathbf{u},90,\mathbf{v},0})}{90.90}.\theta_1.\theta_2 + \bar{\tilde{q}}_i^{\mathbf{u},0,\mathbf{v},0} \quad (7)$$

## 2.4. Validation of the multiple calibration method

To test the multiple calibration method, four wireless sensor nodes SN have been designed to measure the right upper limb joint angles. Each SN is composed of a System in Package BNO055 from Bosch company integrating an IMU consisted of a triaxial 14-bit accelerometer with ranges switchable from ±2g to ±16g, a triaxial 16-bit gyroscope with ranges switchable from ±125°/s to ±2000°/s and a triaxial geomagnetic sensor which can detect ±1300µT in X and Y axes while up to ±2500µT in Z axis with a magnetic resolution around 0.3µT. A 32-bit microcontroller running the sensor fusion software is also integrated. The circuit BNO055 was configured in the fusion mode such that it provided absolute orientation, i.e., sensor orientation with respect to earth coordinate system. Compared to two other typical consumer-grade attitude and heading reference systems (AHRS) (MPU-9150 from InvenSense, X-NUCLEO-1KS01A1 from STMicroelectronics), it displayed the best static and dynamic performances. Attitude measurement obtained from BNO055 showed accuracy of 1.4°, 0.8° and 4.6° for roll, pitch and yaw, respectively [32].

An ATmega328 controller was also used first to acquire data from sensors through the $I^2C$ serial bus then to communicate with an NRF2401 wireless transmission module. The emitting nodes share the same receiving node which ensures data transmission to PC (See Fig. 4). Another possibility consists in using a System on Chip SoC which integrates in the same module the microcontroller and the wireless transceiver, e.g., ESP32s series from Espressif Inc. (single or dual-core module with Wi-Fi & dual-mode Blutooth).

FIGURE 4 HERE

As a proof-of-concept, an upper limb mechanical model composed of three adjacent rigid body segments was designed to test the proposed method under controlled conditions. The upper arm segment is linked to a fixed body through a 3-DoF joint (shoulder) at one end and to the forearm segment through a 2-DoF joint (elbow) at the other end. Elbow FE is obtained by means of a hinge joint whereas two pipes (white and grey on Fig. 5a) with two different diameters were used in the forearm segment to ensure the second DoF movement (pronation-supination PS). Another hinge joint (wrist) is used to link the forearm and the hand segments. A magnetic rotary encoder (0.08° resolution), taken as a reference, was also placed at the elbow joint to measure elbow FE angle and transmit wirelessly the data via an NRF2401 module.

FIGURE 5 HERE

Three sensor nodes SN1, SN3 and SN4 were attached with a double-sided tape to the upper arm, forearm and hand segments axes respectively as illustrated in fig 5b. They were placed so as their long axes were parallel to the segments axes. The fourth one, i.e., SN2 was also attached with a double-sided tape to a 5 mL plastic syringe whose one extremity was attached to the upper arm and the other extremity to the forearm segment via a rod. Initially, when the elbow is fully extended, the piston is parallel to the upper arm segment, so SN2 is aligned with SN1. As soon as the elbow is flexed, the piston induces a misalignment of SN2 (See Fig. 5b) that increases gradually with respect to SN1 till elbow joint reaches 90°. The piston ensures a controlled and repeatable misalignment of SN2 with respect to the upper arm segment. The proposed calibration method was applied to elbow FE between 0° and 90°. SN1 was used during the calibration session to get the upper arm segment orientation without misalignment. The joint angle was obtained from SN2 and SN3 data. Once the calibration postures achieved, the alignment differences $\tilde{q}_i^j$ were calculated between SN1 and SN2 orientations for each posture presented in Fig. 2.

Since elbow flexion disturbed only the SN2 alignment with respect to the upper arm segment, a linear interpolation was applied to correct the orientation of the upper arm segment.

### 2.5. Right upper limb joint angle measures

For a more realistic evaluation of the method, experimental measures have been carried out on a healthy male subject (age: 27 years, height: 175cm, mass: 65 kg). Four SNs were attached on the right upper limb segments as illustrated on the photograph of Fig. 6.

FIGURE 6 HERE

One sensor node was attached on the subject torso and three others on the right upper limb using elastic bracelets. SN placements shown in Fig. 6 are the same as the IMU sensors used in [4]. SN1 was placed on the flat part of the sternum, and SN2 and SN3 were respectively attached to the outer side of the arm and near to the wrist on the forearm. SN4 was fixed dorsally on the hand. The technical calibration was performed by adjusting manually SNs positions in order to visually align their local frames with the associated segment anatomical frames. The subject was asked to successively perform the 21 calibration postures in the same way as presented in Fig.2. The correctness of each posture is checked by an operator before executing to the next one. The subject remained static during several seconds and a calibration session duration did not exceed five minutes. OMCS system based on four Bonita infrared cameras from Vicon was used as a reference system; this system can provide precision down to 0.5mm of translation and 0.5° of rotation using 9mm markers. Reflective markers were placed on anatomical landmarks according to the methodology of Cooper et al. [34]. Both of SNs and video systems were synchronized and operated at a sampling rate of 50Hz. The subject in the neutral position was instructed to achieve three different movements not fastly (average angular speed around 60°/s): (i) forearm PS when elbow is 90° flexed in the sagittal plane; (ii) maximum elbow FE in the sagittal plane; (iii) Shoulder internal external-rotation IER in the horizontal plane when the elbow is 90° flexed in the sagittal plane.

# 3. Results

## 3.1. Three-linked rigid segment body

Several elbow FE movements have been carried out on the three-linked rigid segment body representing the upper arm, the forearm and the hand. Elbow FE angle versus time before and after calibration is depicted in Fig. 7. The reference angle from the magnetic encoder is also represented on the same figure in black dashed line. The bottom curves plotted in red dashed and blue solid lines refer to the error value between the angles deduced from SNs and those gotten from the encoder before and after calibration, respectively. Initially, the three SNs were aligned with the body's segments, so the joint angles values from IMUs and the reference system were the same and equal to zero. As the elbow flexion angle value increases, the alignment error raises gradually to reach a maximal value of 20.7° when the elbow is 90° flexed with a root mean square error RMSE equal to 8.3°. After correction, both the maximal error value and RMSE decreased to 6.1°and 2.2° respectively.

FIGURE 7 HERE

## 3.2. Human joint angle estimation

### 3.2.1. Alignment differences during the calibration

The impact of each movement about the upper limb joint DoFs considered during the calibration session is investigated by computing the median, quartiles, and range of the alignment differences $\tilde{q}_i^j$ for all postures. The SN4 alignment difference varies between 4.8° and 43.5° with a mean value equal to 18°. A closer analysis revealed that the alignment difference is mainly associated with wrist FE. SN3 alignment difference varies between 4.3° and 32.5° with a mean value equal to 15.5°. The alignment difference is mostly associated with elbow FE and forearm PS. The most affected sensor node is the SN2 as presented in Fig 8 where alignment difference ranges from the smallest variation 3.9° to 53.8° with a mean value equal to 23.6°. The alignment difference is predominantly related to elbow FE and shoulder IER.

FIGURE 8 HERE

### 3.2.2. Correction of the forearm pronation-supination movement

The subject performed several forearm PS when the elbow is 90°-flexed with SNs placed as illustrated in Fig. 6. Fig. 9 shows elbow joint angle during forearm PS as a function of time from both SNs and optical systems. Black dashed line curve is obtained from OMCS system while the red dashed line curve corresponds to angle data from SN3 with respect to SN2. It can be noticed that SN3 joint angle is almost the same as the reference angle from OMCS system with a mean error value equal to 1.0° and max error value of 2°. Still, the correction of the forearm PS can be useful if another placement of the SN is adopted (see Supplementary Material). Whatever the placement of the SN on the forearm, it can be noticed that the errors at the beginning and ending of the movement are tending to zero demonstrating initially aligned IMUs in the upper arm and forearm segments.

FIGURE 9 HERE

### 3.2.3. Correction of the maximum elbow FE movement

The subject was asked to perform successive cycles of maximum right elbow FE (range of motion equal to 140°) and FE angle was measured simultaneously with SNs and the optical reference system.

FIGURE 10 HERE

FE angle values obtained from misaligned SNs and plotted in red dashed line on Fig. 10 deviate from the reference angles plotted in black dashed line on the same figure during the elbow FE movements. The multiple calibration has corrected quite well the angle values obtained from SNs since the associated curve (blue solid line) in Fig. 10 is close to the reference one. The maximal error value decreased from 23° (RMSE=9°) before correction to 12° (RMSE=4°) after correction. The mean error value decreased from 6° (SD=7°) before correction to 0° (SD=4°) after correction. Again, it can be noticed that the errors

at the beginning and ending of the movement are tending to zero demonstrating initially aligned IMUs in the upper arm and forearm segments.

#### 3.2.4. Correction of the Shoulder internal - external rotation movement

The right shoulder IER movement was performed in the horizontal plane when the elbow joint is 90°-flexed. The red dashed line curve in Fig.11 corresponding to shoulder IER angle before correction diverge a lot when comparing to the reference angles plotted in black dashed line. The results obtained from SNs after correction (blue solid line) are still different but improved when compared to before correction (red dashed line).

FIGURE 11 HERE

Error up to 30° was obtained before correction with a mean value of 8° (SD=11°). After correction, the error was reduced to less than 15° with a mean value equal to 3° (SD=7°). Again, it can be noticed that the errors at the beginning and ending of the movement are tending to zero demonstrating initially aligned IMUs in the thorax and upper arm segments.

## 4. Discussion

The proposed compensation method is based on a multiple sensor-to-segment calibration. It is assumed that the alignment between sensor and segment is impacted by the joint movement. Twenty-one predefined static postures are necessary to study the misalignment -non constant in time- for the all of the shoulder, elbow and wrist joints movements with a calibration session not exceeding five minutes. This number of static predefined postures could be cumbersome in a clinical context. If only one joint is studied at the time, the number of postures can be highly reduced (to two) as it was the case for the application on the mechanical model (see Fig.5). The purpose of displaying the 21 postures is to allow the reader to pick the ones of interest for its own research.

Concerning the alignment differences during the multiple calibration, the IMUs placed on the upper limb are not impacted in the same way according to the different joint orientations. SN4 alignment is

significantly modified by wrist FE, SN3 by elbow FE or forearm PS, and SN2 by elbow FE as well as shoulder IER. The impact of the elbow FE and shoulder IER on the movement of skin markers was already reported in the literature [18, 35]. This observation justifies the use of an interpolation based on joint angles for the correction of the IMU frame orientation. Few studies have quantified the STA on the upper limb using bone pins or fluoroscopy [36]. Skin markers placed on the humerus can undergo a displacement up to 4 cm with respect to the bone during arm abduction. The main movement pattern of the marker displacement is also a rotation of the marker cluster [16] which implicates potential large errors when IMUs are used. As a matter of fact, in the present study, the differences of IMU alignment reached 53° for the upper arm.

Concerning the correction of the IMU frame orientation, the tests performed on the upper limb mechanical model confirmed the feasibility and efficiency of the proposed method to compensate for an ongoing misalignment when IMUs were initially aligned.

The graphs corresponding to the subject movements of forearm PS, elbow FE and shoulder IER revealed two results relative to the IMUs. First, a good initial alignment has been achieved with the technical calibration during the calibration session as reported in the literature [4, 10]. However, other types of calibration such as anatomical calibration may be considered [19, 37, 38]. Second, a correct placement of SN3 on the forearm is important as this sensor can provide an accurate elbow PS measurement without correction. However, with SN3 placed far from the wrist, when compared to the data obtained from the optical OMCS system, maximal alignment error values up to 30° are reached during the forearm PS. Elbow FE angle has been measured on the mechanical upper arm as well as on a subject. FE angle values obtained from the multiple calibration are somehow underestimated in the former case while they are slightly overestimated in the second case. These effects may be due to an error associated with the segment placement at 0° or 90° during the calibration session. Results accuracy estimated as RMSE for elbow FE and PS were found to be equal to 4°. This value is significantly lower than those reported in the literature from static calibration with misalignment constant in time ($11° \leq RMSE \leq 24°$) [4].The maximal error value for shoulder IER initially equal to 30° confirms that this movement is the most affected by STA. Such a result is consistent with the value of the parameter K defined by Cutti et al. [18] to measure STA effect on humeral internal/external rotation. This error decreased more than

50% (SD=7°) after correction. For the three movements studied, the errors were then reduced to less than 15° in maximum (less than 5° in average) for both elbow and shoulder joints after correction. The mean error value of 5° could be considered as a good result especially for shoulder's movements compared to those already reported in the literature [3, 4]. Low-cost consumer-grade motion sensors with quite good performances were used in this study. Better results would have been expected if industrial-grade motion sensors such as MTi-300 from Xsens Inc. which shows better orientation accuracy [32].

It is worth noticing that the definition of the segment axes from the OMCS system in the present work follows the methodology of Cooper et al. [34] This choice was made in order to limit the number of skin marker and avoid occlusion (i.e., typically the medial epicondyle) in the different postures. It seems that with this definition of the segment axes, the technical calibration of the IMUs provides better results than previously reported in the literature [3, 4], as demonstrated by the limited errors values (close to zero) at the beginning and ending of the studied movements whereas RMSE was found to vary between 15.8° and 18.7° for elbow FE and PS, and up to 23.4° for shoulder IER in [4].

Though the misalignment correction was based on interpolation between alignment differences related to 0° and 90° joint angles, this method showed good results for intermediate values of joint angles in 0-90° range. Even if the joint angle exceeds 90° as in the maximal elbow FE, the proposed multiple calibration revealed good results by extrapolation. Quaternions rather than rotation matrices or Euler angles are more suitable for interpolation. Moreover, the interpolation is based on joint angles and it has been established that STA effect is correlated to the joint angles [38, 39]. In the present work, the misalignment due to STA is assumed to behave linearly during the multiple calibration. Similar assumption was proposed in a multiple anatomical landmark calibration for optimal bone pose estimation for lower limbs [7]. STA behavior was fairly described by a linear model as function of the joint angles on pin-marker data and skin-marker data from lower limbs [15, 40-42]. In real time, STA is depending on the movement of the whole limb. The choice of considering only one joint angle was driven by the number of postures needed to calibrate the model. If a multi-linear model is used, more than 21 postures are required. Moreover, multi-linear STA models based on three to four joint angles for the lower limb have been proposed in the literature, but they necessitate calibration with bone pin

data in order to identify the model parameters [15, 42]. In the method presented in this work, only linear or bi-linear interpolation is considered and the calibration is performed non-invasively with 21 postures during the calibration session. Interpolation of higher order would have necessitated additional postures. Another possibility to compensate for the STA, yet more rarely applied to IMUs, is to introduce joint constraints and to perform a multibody kinematics optimization [43].

The present study shows some limitations: (i) the measurements were carried out on an upper limb mechanical model taken as a proof-of-concept and only on one healthy subject knowing that STA is subject and task specific [44]. However, it has been demonstrated that a same STA model (a linear function of the joint angle) can be calibrated on different subjects [15, 45]; (ii) the performance of the proposed multiple calibration has been investigated on three active movements of the upper limb during which only one angle varies. These movements are performed at low velocities which may tend to minimize the STA; (iii) the shoulder complex is simplified and the scapula movement has not been considered in this work; (iv) the STA were not measured (i.e. using bone pins or fluoroscopy) but indirectly estimated. Using the OMCS as the reference implicitly assumes that STA effects are weaker on the markers placed on the anatomical landmarks than on the IMUs orientations. This remains to be demonstrated. The differences in the IMU alignment during the calibration step rely on the postures which are assumed to represent ideal 0° or 90° joint angles. The joint angle values obtained from IMUs are then compared to those from OMCS considered as a reference. This is a standard procedure [3-5, 10, 25, 27] but the true joint angles remain unknown.

## 5. Conclusion

The multiple calibration proposed in this work is an IMU based sensor-to-segment calibration method which can be considered as an extension of the double calibration: it is applied to IMUs orientation rather than marker cluster deformation and considers two joint angles rather than only one. The proposed procedure allows for the identification of the sensor frame misalignment and of the joint axes of movement that cause it. Once identified, the sensor frame misalignments can be corrected during the movement with promising results showed in this proof-of-concept study. In future work, another study

shall be undertaken on the multiple calibration of IMUs which takes into account the scapula movement and consider more complex movements performed by several subjects.

References


[1] Rowe PJ, Myles CM, Hillmann SJ, Hazlewood ME (2001) Validation of flexible electrogoniometry as a measure of joint kinematics. Physiotherapy 87:479-488. https://doi.org/10.1016/S0031-9406(05)60695-5

[2] Alvarez D, Alvarez JC, Gonzalez RC, Lopez AM (2015) Upper limb joint angle measurement in occupational health. Comput Meth Biomech Biomed Eng 19:159-170. https://doi.org/10.1080/10255842.2014.997718

[3] Robert-Lachaine X, Mecheri H, Larue C, Plamondon A (2017) Validation of inertial measurement units with an optoelectronic system for whole-body motion analysis. Med Biol Eng Comput 55:609-619. https://doi.org/10.1007/s11517-016-1537-2

[4] Bouvier B, Duprey S, Claudon L, Dumas R, Savescu A (2015) Upper Limb Kinecmatics Using Inertial and Magnetic Sensors: Comparaison of Sensor-to-Segment Calibrations. Sensors 15:18813-33. H ttps://doi.org/ doi: 10.3390/s150818813.

[5] Bolink SAAN, Naisas H, Senden R, Essers H, Heyligers IC, Meijer K, Grimm B (2016) Validity of an inertial measurement unit to assess pelvic orientation angles during gait, sit-stand transfers, and step-up transfers: Comparison with an optoelectronic motion capture system. Med Eng Phys 38:225-231. https://doi.org/10.1016/j.medengphy.2015.11.009

[6] Cappozzo A, Della Croce U, Lardini A, Chiari L (2005) Human movement analysis using stereophotogrammetry Part1 : theorical background. Gait and Posture 21:186-196 https://doi.org/10.1016/j.gaitpost.2004.01.010

[7] Cappello A, Cappozzo A, La Palombara PF, Lucchetti L, Leardini A (1997) Multiple anatomical landmark calibration for optimal bone pose estimation. Hum Movement Sci 16:259-274. https://doi.org/10.1016/S0167-9457(96)00055-3

[8] Qureshi U and Golnaraghi F (2017) An algorithm for the in field calibration of a MEMS IMU. IEEE Sens J 17:7479-7486.
https://doi.org/ 10.1109/JSEN.2017.2751572

[9] Kopacik A, Kajanek P, Liptak I (2016) Systematic Error Elimination Using Additive Measurements and Combination of Two Low Cost. IEEE Sens J 16:6239-6248.
https://doi.org/ 10.1109/JSEN.2016.2581200

[10] Cutti AG., Giovanardi A, Rocchi L, Davalli A, Sacchetti R (2008) Ambulatory measurement of shoulder and elbow kinematics through inertial and magnetic sensors. Med Biol Eng Comput 46:169-178.
https://doi.org/10.1007/s11517-007-0296-5

[11] Vargas-Valencia L, Elias A, Rocon E, Bastos-Filho T, Frizera A (2016) An IMU-to-Body Alignment Method Applied to Human Gait Analysis. Sensors 12:2090-2107.
https://doi.org/doi:10.3390/s16122090

[12] de Vries WHK, Veeger HEJ, Cutti AG, Baten C,. Van der Helm FCT (2010) Functionally interpretable local coordinate systems for the upper extremity using inertial & magnetic measurement systems. J Biomech 43:1983-1988.
https://doi.org/10.1016/j.jbiomech.2010.03.007

[13] Robert-Lachaine X, Mecheri H, Larue C., Plamondon A (2017) Accuracy and repeatability of single-pose calibration of inertial measurement units for whole-body motion. Gait Posture 54:80-86. https://doi.org/10.1016/j.gaitpost.2017.02.029

[14] Lach E (2016) Evaluation of Automatic Calibration Method for Motion Tracking Using Magnetic and Inertial Sensors, In: Piętka E., Badura P., Kawa J., Wieclawek W. (eds) Information Technologies in Medicine. ITiB 2016. Advances in Intelligent Systems and Computing, vol 472. Springer, Cham.
https://doi.org/10.1007/978-3-319-39904-1_30

[15] Camomilla V, Bonci T, Dumas R, Cheze L, Cappozzo A (2015) A model of the soft tissue artefact rigid component. Journal of Biomechanics 48:752-1759. https://doi.org/10.1016/j.jbiomech.2015.05.007

[16] Blache Y, Dumas R, Lundberg A, Begon M (2017) Main component of soft tissue artifact of the upper-limbs with respect to different functional, daily life and sports movements. J Biomech 62:39-46. https://doi.org/10.1016/j.jbiomech.2016.10.019

[17] Cutti AG, Cappello A, Davalli A (2006) In vivo validation of a new technique that compensates for soft tissue artefact in the upper-arm: Preleminary results. Clin Biomech 21:S13-S19. https://doi.org/10.1016/j.clinbiomech.2005.09.018

[18] Cutti AG, Paolini G, Troncossi M, Cappello A, Davalli A (2005) Soft tissue artefact assessment in humeral axial rotation. Gait Posture 21:341-359. https://doi.org/10.1016/j.clinbiomech.2005.09.018

[19] Cappello A, Stagni R, Fantozzi S, Leardini A (2005) Soft Tissue Artifact Compensation in Knee Kinematics by Double Anatomical Landmark Calibration: Performance of a Novel Method During Selected Motor Tasks. IEEE Trans. on Biomed Eng 52:992-998. https://doi.org/10.1109/TBME.2005.846728

[20] Meng D, Shoepe T, Vejarano G (2016) Accuracy Improvement on the Measurement of Human-Joint Angles. IEEE J Biomed Health Informatics 20:498-507. https://doi.org/10.1109/JBHI.2015.2394467

[21] Camomilla V, Dumas R, Cappozzo A (2017) Human movement analysis: The soft tissue artefact issue. J Biomech 62:1-4. https://doi.org/10.1109/JBHI.2015.2394467

[22] Brochard S, Lempereur M, Rémy-Néris O (2011) Double calibration: An accurate, reliable and easy-to-use method for 3D scapular motion analysis. J Biomech 44:751-754. https://doi.org/10.1016/j.jbiomech.2010.11.017

[23] Ricci L, Formica D, Sparaci L, Lasorsa FR, Taffoni F, Tamilia E, Guglielmelli E (2014) A new calibration methodology for thorax and upper limbs motion capture in children using magneto and inertial sensors. Sensors 14: 1057-1072. https://doi.org/10.3390/s140101057.

[24] Prayudi I and Kim D (2012) Design and Implementation of IMU-based Human Arm Motion Capture System, in Proc. IEEE International Conference on Mechatronics and Automation. https://doi.org/ 10.1109/ICMA.2012.6283221.

[25] Miezal M, Taetz B, Bleser G (2016) On Inertial Body Tracking in the Presence of Model Calibration Errors. Sensors. https://doi.org/10.3390/s16071132.

[26] Taetz B, Bleser G, Miezal M (2016) Towards Self-Calibrating Inertial Body Motion Capture, in Proc. IEEE 19th International Conference on Information Fusion (FUSION):1751-1759

[27] Muller P, Begin M-A, Schauer T, Seel T (2016) Alignment-Free, Self-Calibrating Elbow Angles Measurement using Inertial Sensors. IEEE J Biomed Health Informatics 21:312-319. https://doi.org/10.1109/JBHI.2016.2639537

[28] Palermo E, Rossi S, Marini F, Patane F, Cappa P (2014) Experimental evaluation of accuracy and repeatability of a novel body-to-sensor calibration procedure for inertial sensor-based gait analysis. Measurement 52:145-155. https://doi.org/10.1016/j.measurement.2014.03.004

[29] Luinge HJ, Veltink PH, Baten CTM (2007) Ambulatory measurement of arm orientation. J Biomech 40:78–85. https://doi.org/10.1016/j.jbiomech.2005.11.011

[30] Ligorio G, Zanotto D, Sabatini AM, Agrawal SK (2017) A novel functional calibration method for real-time elbow joint angles estimation with magnetic-inertial sensors. J Biomech 54:106-110. https://doi.org/10.1016/j.jbiomech.2017.01.024

[31] Wu G, Van der Helm FCT, Veeger HEJ et al. (2005) ISB recommendation on definitions of joint coordinate systems of various joints for the reporting of human joint motion-Part II: shoulder, elbow, wrist and hand. J Biomech 38:981-992. https://doi.org/10.1016/j.jbiomech.2004.05.042

[32] Lin Z, Xiong Y, Dai H, Xia X (2017) An Experimental Performance Evaluation of the Orientation Accuracy of Four Nine-Axis MEMS Motion Sensors. in Proc. IEEE 5th International Conference on Enterprise Systems ICES:185-189. https://doi.org/10.1109/ES.2017.37

[33] Bosch Sensortech (2016) Datasheet BNO055 Intelligent 9-axis absolute orientation sensor. Available via https://ae-bst.resource.bosch.com/media/_tech/media/datasheets/BST-BNO055-DS000.pdf. Accessed 15 Jun 2019.

[34] Cooper RA, Boninger ML, Shimada SD, Lawrence BM (1999) Glenohumeral joint kinematics and kinetics for three coordinate system representing during wheelchair propulsion. American J Phys. Med Rehabil 78:435-446.

[35] Cao L, Masuda T, Morita S (2007) Compensation for the Effect of Soft Tissue Artefact on Humeral Axial Rotation Angle. J Med Dent Sci 54:1-7. https://doi.org/10.11480/jmds.540101

[36] Cereatti A., Bonci T., Akbarshahi M., Aminian K., Barre A et al. (2017) Standardization proposal of soft tissue artefact description for data sharing in human motion measurements. J Biomech 62:5-13. https://doi.org/10.1016/j.jbiomech.2017.02.004

[37] Donati M, Camomilla V, Vannozzi G, Cappozzo A (2007) Enhanced anatomical calibration in human movement analysis. Gait Posture 26:179-185. https://doi.org/10.1016/j.gaitpost.2007.04.009

[38] Picerno P, Cereatti A, Cappozzo A (2008) Joint kinematics estimate using wearable inertial and magnetic sensing modules. Gait Posture 28:588-595. https://doi.org/10.1016/j.gaitpost.2008.04.003

[39] Cappozzo A, Catani F, Leardini A, Benedetti MG, Croce UD (1996) Position and orientation in space of bones during movement: experimental artefacts. Clin Biomech 11:90-100. https://doi.org/10.1016/0268-0033(95)00046-1

[40] Barre A, Aissaoui R, Aminian K, Dumas R (2017) Assessment of the lower limb soft tissue artefact at marker-cluster level with a high-density marker set during walking. J Biomech 62:21-26. https://doi.org/10.1016/j.jbiomech.2017.04.036

[41] Andersen MS, Damsgaard M, Rasmussen J, Ramsey DK, Benoit DL (2012) A linear soft tissue artefact model for human movement analysis: Proof of concept using in vivo data. Gait Posture 35:606–611.

https://doi.org/10.1016/j.gaitpost.2011.11.032

[42] Bonci T, Camomilla V, Dumas R, Cheze L, Cappozzo A (2014) A soft tissue aretefact model driven by proximal and distal joint kinematics. J Biomech 47:2354-2361. https://doi.org/10.1016/j.jbiomech.2017.04.036

[43] Begon M, Andersen MS, Dumas R (2018) Multibody kinematics optimization for the estimation of upper and lower limb human joint kinematics. J Biomech Eng 140: 0308011-11. https://doi.org/10.1115/1.4038741

[44] Camomilla V, Bonci T, Cappozzo A (2017) Soft tissue displacement over pelvic anatomical landmarks during 3-D hip movements. J Biomech 62:14-20. https://doi.org/10.1016/j.jbiomech.2017.01.013

[45] Bonnet V, Richard V, Camomilla V, Venture G, Cappozzo A, Dumas R (2017) Joint kinematics estimation using a multi-body kinematics optimisation and an extended Kalman filter, and embedding a soft tissue artefact model. J Biomech 62:148-155. https://doi.org/10.1016/j.jbiomech.2017.04.033

Figure captions

**Figure 1** - IMUs and reflective markers placement on the thorax and the right upper limb: (a) Frontal view; (b) Side view; (c) Rear view.

**Figure 2** - Proposed calibration postures in the calibration session.

**Figure 3 -** (a) IMUs' frames ($Xi_j$,$Yi_j$, $Zi_j$) j=1 to 4, associated with IMUi (i=1 to 4); anatomical frames ($Xa_k$,$Ya_k$, $Za_k$) related to the neutral posture (b) and to the right shoulder adduction (c) corresponding to posture 3 in Fig.2; the subscripts T, U, F and H stand for the thorax, the upper arm, the forearm and the hand, respectively.

**Figure 4 -** Block diagram of a wireless sensor node SN (left); Schematics of BNO055with I2C interface (right) [33].

**Figure 5 -** Three-linked rigid segment body with attached plastic syringe without (a) or with a wireless sensors nodes SNs mounted on the three segments.

**Figure 6 -** Sensor nodes and reflective markers placement on right upper limb and thorax.

**Figure 7 -** Upper-limb-mechanical-model elbow FE angle (top) and error (bottom) versus time before calibration (red dashed line) and after calibration (blue solid line); from encoder (black dashed line),

**Figure 8 –** Alignment difference variation during calibration postures for each attached sensor node.

**Figure 9 -** Right elbow PS angle (top) and error (bottom) versus time without correction (red dashed line); from OMCS (black dashed line).

**Figure 10 -** Maximum right elbow FE angle (top) and error (bottom) versus time before correction (red dashed line) and after correction (blue solid line); from OMCS (black dashed line).

**Figure 11 -** Right shoulder IER joint angle (top) and error (bottom) versus time from SNs before correction (red dashed line) and after correction (blue solid line); from OMCS (black dashed line).

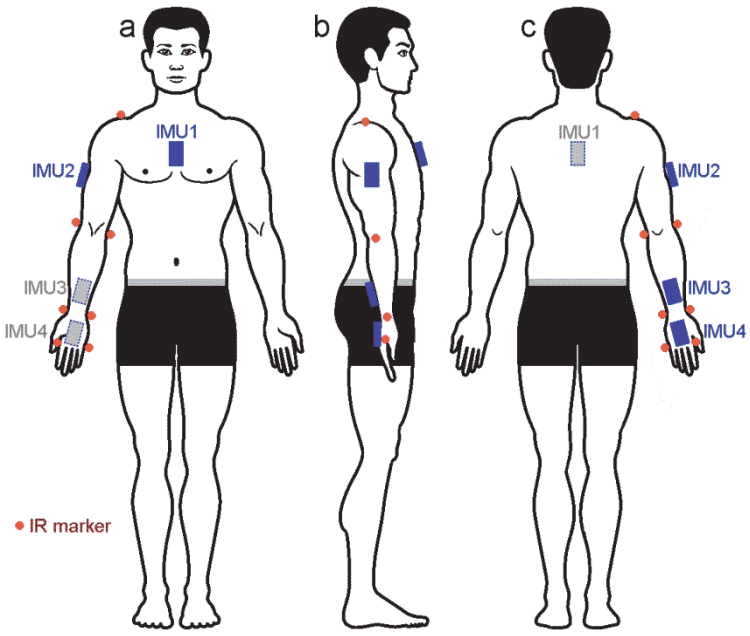


Figure 1

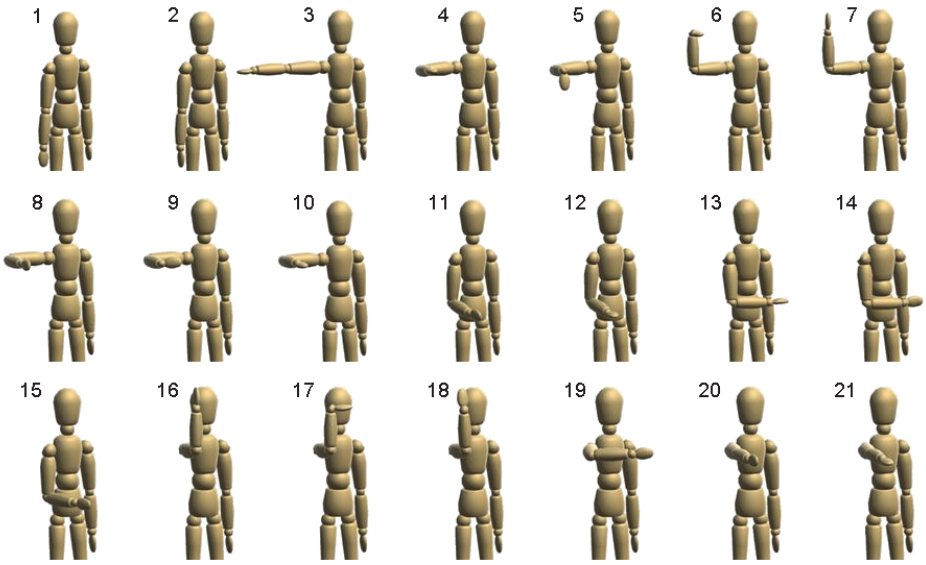


Figure 2

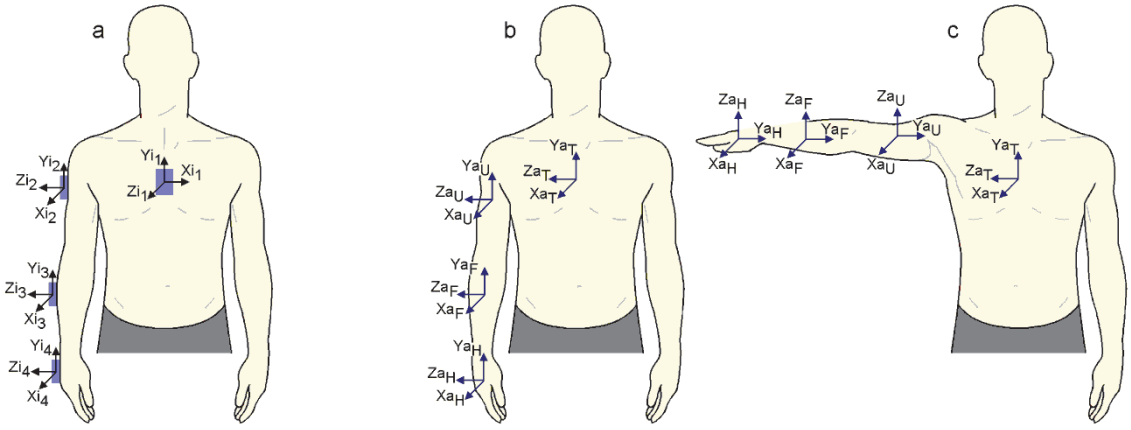


Figure 3

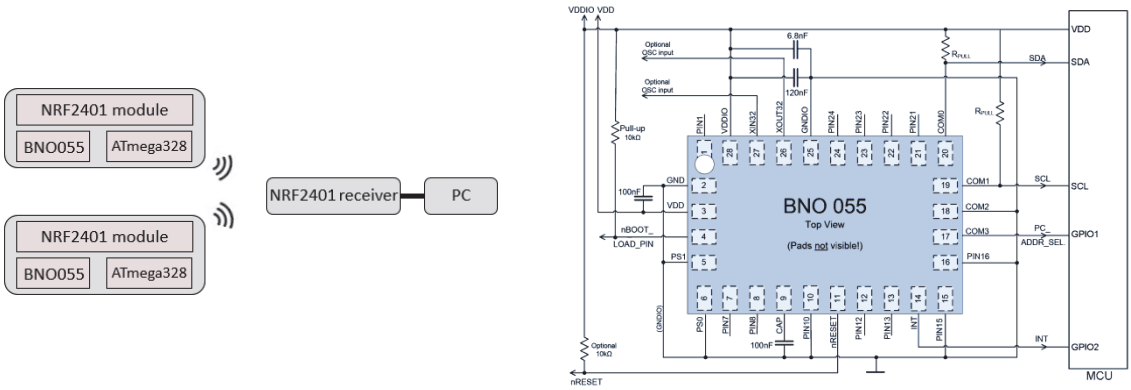


Figure 4

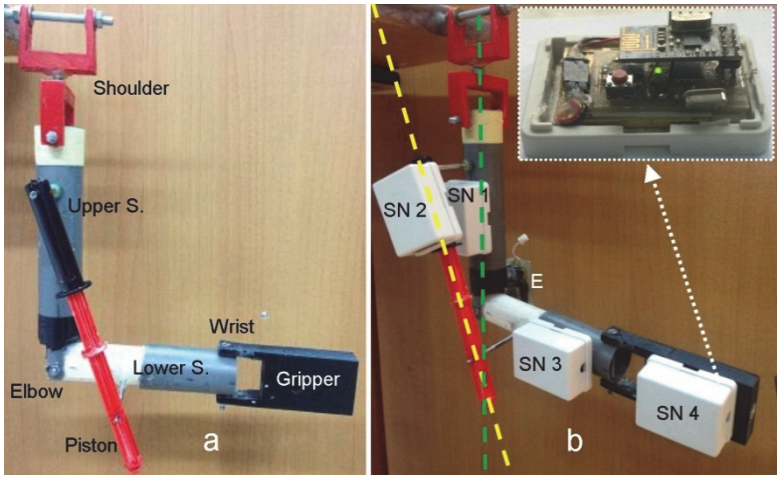


Figure 5

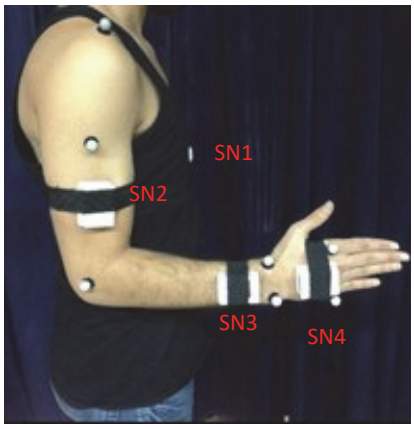


Figure 6

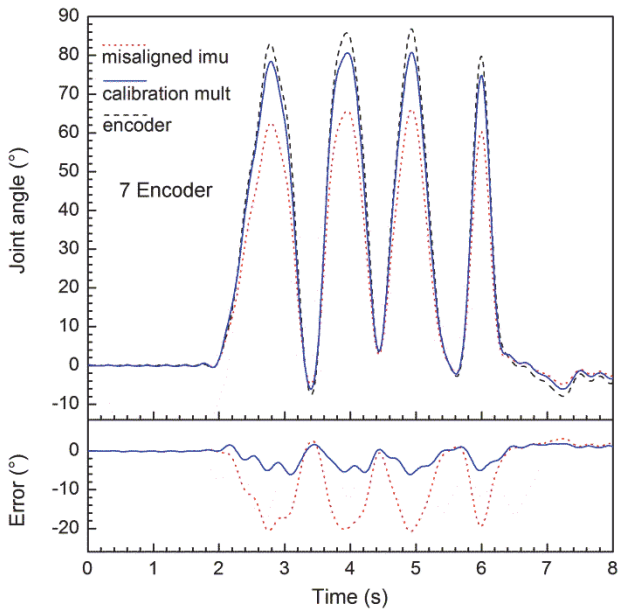


Figure 7

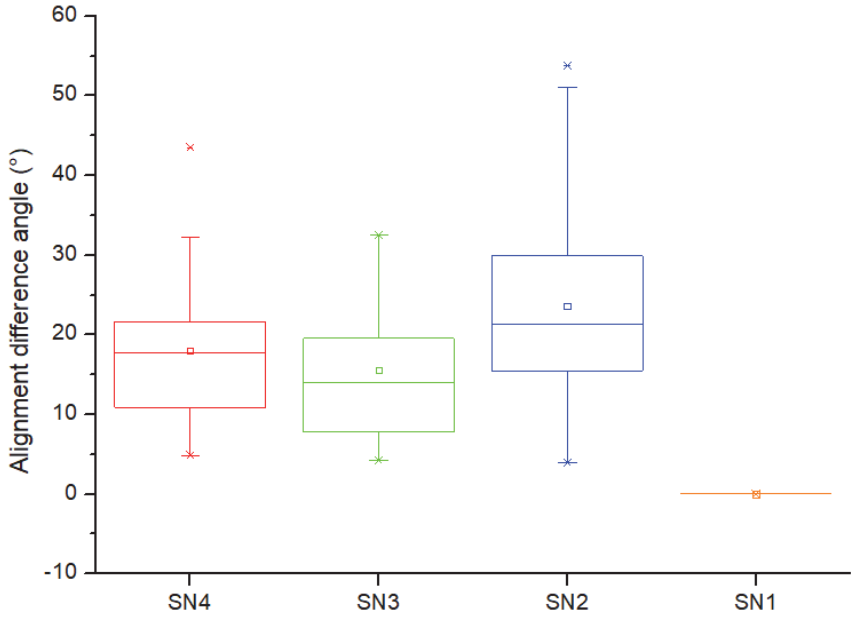


Figure 8

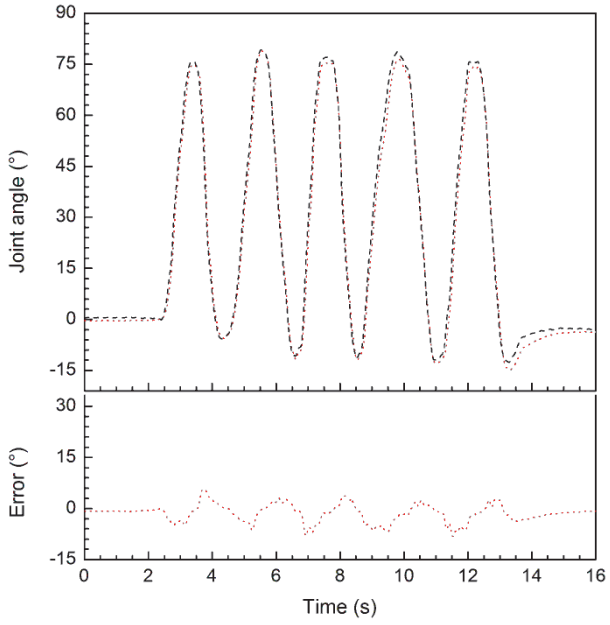


Figure 9

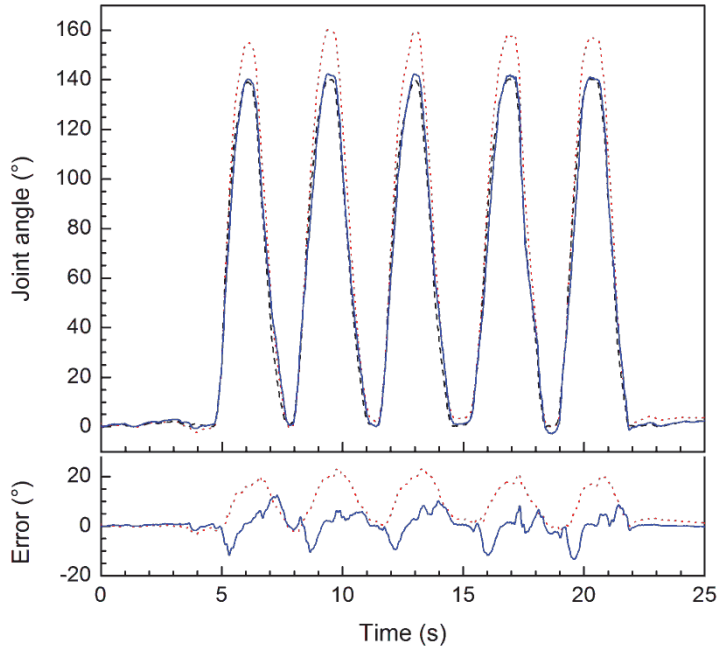


Figure 10

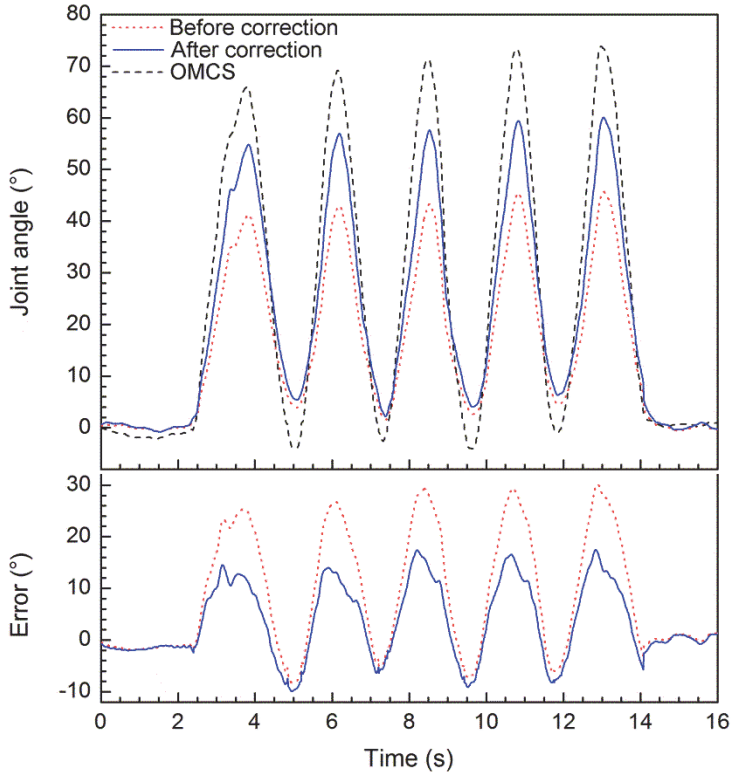


Figure 11

## Authors' Biography

Mahdi Zabat MS is currently a PhD student at University of Science and Technology Houari Boumediene, Algiers, Algeria. His current research focuses on human joint angle measurement with embedded systems.

Amina Ababou PhD is Professor at University of Science and Technology Houari Boumediene, Algiers, Algeria. Her research interests include human movement analysis, wireless sensors & ambulatory systems.

Noureddine Ababou PhD is Assistant Professor at University of Science and Technology Houari Boumediene, Algiers, Algeria. His main research interests include human motricity and instrumentation.

Raphaël Dumas PhD is currently Senior Researcher at IFSTTAR Lyon, France. He is a member of the Francophone Society of Biomechanics (SB) and Francophone Society of Motion Analysis in Children and Adults (SOFAMEA). His research interests include 3D motion analysis & computational biomechanics.